Molecular-beam epitaxy growth and properties of $Be_xZn_{1-x}Te$ alloys for optoelectronic devices

O. Maksimov,[a] Martin Muñoz, and M. C. Tamargo[b]
New York State Center for Advanced Technology on Ultrafast Photonics, Center for Analysis of Structures and Interfaces, and Department of Chemistry, City College of CUNY, New York, New York 10031

J. Lau and G. F. Neumark
School of Mines and Department of Applied Physics, Columbia University, New York, New York 10027

(Received 24 October 2001; accepted 25 February 2002)

We report the molecular-beam epitaxy growth and characterization of $Be_xZn_{1-x}Te$ epitaxial layers on (100) InP substrates. $Be_xZn_{1-x}Te$ layers with x varying from 0 to 0.58 were grown. Good control of the composition is achieved by adjusting either the Be or the Zn cell temperatures. The layers exhibit high-crystalline quality, as established by double crystal x-ray diffraction and etch pit density measurements. Narrow x-ray rocking curves with a linewidth of 72 arcsec and etch pit density of 5×10^5 cm^{-2} are obtained for the $Be_xZn_{1-x}Te$ layers closely lattice matched to the InP substrate. $Be_xZn_{1-x}Te$ layers under tensile strain, which have higher BeTe content, exhibit slower degradation of the crystalline quality as a function of lattice mismatch than layers under compressive strain. The lattice-hardening properties of BeTe are proposed to be the reason for this behavior. © *2002 American Vacuum Society.* [DOI: 10.1116/1.1470515]

I. INTRODUCTION

In the past several years $Zn_xCd_yMg_{1-x-y}Se$-based light emitting diodes (LEDs) operating in the visible range of the spectrum have been reported by several research groups.[1–3] These LED structures are grown on InP substrates and utilize lattice-matched $ZnSe_{0.5}Te_{0.5}$ or $Zn_xMg_{1-x}Se_yTe_{1-y}$ as the top p-type contact layers. However, there are drawbacks involved in the use of each of these materials. In the case of $ZnSe_{0.5}Te_{0.5}$, which can be doped p-type to carrier concentration levels in excess of 10^{19} cm^{-3}, absorption of the emitted light by the contact layer limits the performance of surface emitting LEDs.[4] When $Zn_xMg_{1-x}Se_yTe_{1-y}$ layers with band gaps of 3.1 eV are used, the maximum free-hole concentration is in the low 10^{18} cm^{-3}, making the formation of ohmic contacts more difficult.[2]

A promising alternative material for use as a p-type contact layer is $Be_xZn_{1-x}Te$. It can be lattice matched to the InP substrate with a BeTe mole fraction of ~0.48 and it can be doped p-type to the 10^{19} cm^{-3} level.[5,6] Also, since $Be_{0.48}Zn_{0.52}Te$ is an indirect semiconductor with a direct band-gap energy of 3.14 eV, it does not absorb light in the visible range of the spectrum.[7] However, there is no systematic study of the growth and properties of this material system.

In this article, we report the molecular-beam epitaxy (MBE) growth and characterization of $Be_xZn_{1-x}Te$ epitaxial layers on InP (100) substrates. The dependence of the Be content on the Be and Zn cell temperatures is investigated and good reproducibility from run to run is observed. Small compositional fluctuations observed in some $Be_xZn_{1-x}Te$ epitaxial layers are explained by slight fluctuations of the substrate temperature. The crystalline properties of the epilayers are studied by double-crystal x-ray diffraction (XRD) and etch pit density (EPD) measurements. Narrow x-ray rocking curves (72–78 arcsec) and low etch pit density (5×10^5 cm^{-2}) are obtained for the closely lattice-matched epilayers indicating high-crystalline quality. The crystalline quality of the $Be_xZn_{1-x}Te$ epilayers under compressive and tensile strain is compared. A slower degradation of the crystalline quality as a function of strain for epilayers under tensile strain compared to epilayers under compressive strain is observed.

II. EXPERIMENTAL DETAILS

$Be_xZn_{1-x}Te$ epilayers were grown in a Riber 2300P MBE system using elemental Be, Zn, and Te sources. This system consists of two growth chambers connected by an ultrahigh vacuum transfer channel. One growth chamber is used for As-based III-V materials and the other is for wide band-gap II-VI materials.

The growth was performed on semi-insulating InP (100) substrates. Prior to use, the substrates were degreased and etched as previously described.[8] The substrates were deoxidized in the III-V chamber by heating to 480 °C with an As flux impinging on the InP surface. A lattice matched $In_{0.53}Ga_{0.47}As$ buffer layer (170 nm) was grown after the deoxidization. The buffer layer was terminated with an As-rich (2×4) surface reconstruction and the samples were transferred in vacuum to the II-VI chamber for the $Be_xZn_{1-x}Te$ growth. Prior to the initiation of the II-VI growth, the samples were heated to 170 °C and the As-terminated III-V surface was exposed to a Zn flux for 40 s (Zn irradiation) to optimize the II-VI/III-V interface quality. $Be_xZn_{1-x}Te$ layers were grown at 270 °C under Te-rich conditions, as characterized by a (2×1) surface reconstruction,[9] with a group-VI to group-II flux ratio of ~3. The

[a]Electronic mail: maksimov@netzero.net
[b]Electronic mail: tamar@sci.ccny.cuny.edu

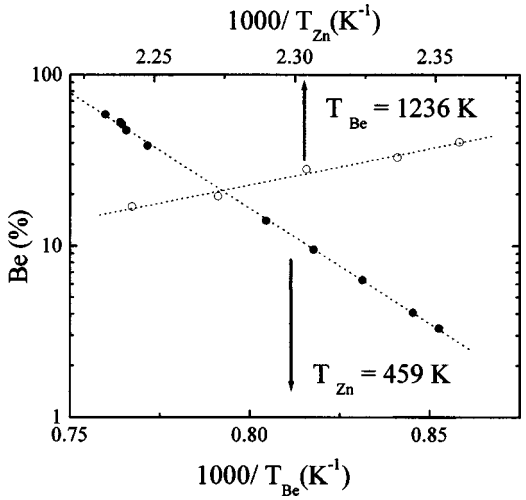

FIG. 1. Dependence of the Be content (x) on the Be (solid circles) and Zn (open circles) cell temperatures for $Be_xZn_{1-x}Te$ alloy. Dashed lines are linear fits.

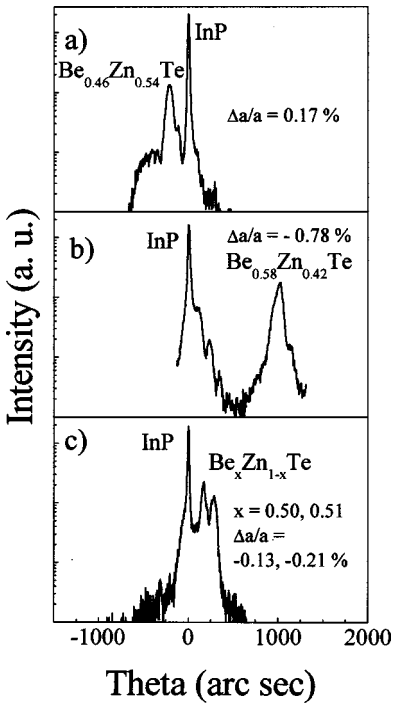

FIG. 2. (004) Double crystal x-ray rocking curves for three $Be_xZn_{1-x}Te$ layers with different composition grown on InP substrates: (a) $Be_{0.46}Zn_{0.54}Te$; (b) $Be_{0.58}Zn_{0.42}Te$; and (c) $Be_xZn_{1-x}Te$ with $x=0.50$ and 0.51.

$Be_xZn_{1-x}Te$ composition was controlled by adjusting the Be and/or Zn cell temperatures, which control Be to Zn flux ratio. The growth rate was around 0.25–0.45 μm/h and the layers were 0.5–0.9 μm thick.

The growth mode and surface reconstruction were monitored *in situ* by reflection high-energy electron diffraction. Lattice constants were measured by single-crystal and double-crystal XRD using Cu $K_{\alpha 1}$ radiation. Alloy composition was estimated from the lattice constant, assuming the validity of Vegard's law and using 6.104 and 5.622 Å as the lattice constants for ZnTe and BeTe, respectively.[10,11]

The layer thickness was measured using a Philtec sectioner. The surface morphology was investigated using a Nomarski microscope and a contact mode atomic force microscope (AFM).

III. RESULTS AND DISCUSSION

The control of the composition during the MBE growth of the $Be_xZn_{1-x}Te$ alloy system was investigated. The composition was varied by adjusting the Be and/or Zn cell temperatures, which control the fluxes of these two species. Two experiments were performed. In the first experiment several samples were grown in which we increased the Be cell temperature with the Zn cell temperature held constant at 183 °C. In the other experiment we decreased the Zn cell temperature with the Be cell temperature held constant at 960 °C. The cell temperature is directly related (exponentially) to the flux of the species, which determines the layer composition. Flux determination is usually based on beam equivalent pressure (BEP) measurements using a flux gauge. However, accurate BEP measurements are difficult for group-II elements, and in particular for Be, so in our experiment we plot the temperature of the source cells. As shown in Fig. 1, the Be content increases linearly on a logarithmic scale with the increase (decrease) in the Be (Zn) cell temperature. Good reproducibility from run to run is observed.

The (004) reflections of the double crystal x-ray rocking curve for $Be_xZn_{1-x}Te$ epilayers with different Be mole fractions are shown in Fig. 2. In all spectra the dominant peak is from the InP substrate and the others originate from the epilayer. In Figs. 2(a) and 2(b), single peaks with full widths at half-maximum (FWHM) of 72 and 91 arcsec, respectively, are observed indicating high-quality material. In a few cases, such as that shown in Fig. 2(c), two closely overlapping peaks related to the $Be_xZn_{1-x}Te$ epilayer are observed. In these cases, similar spectra were obtained from different areas of the wafer suggesting that these do not represent lateral variations in layer composition. We attribute the presence of two closely spaced peaks to the presence of two regions with slightly different Be content ($x=0.50$ and 0.51) as a function of depth. A strong dependence of the $Be_xZn_{1-x}Te$ composition on the growth temperature has previously been reported.[6] For example, in our experiments, we observe that an increase in the growth temperature from 270 to 300 °C results in a compositional change from $x=0.45$ to $x=0.50$. This strong substrate temperature dependence may be due to the fact that, in this temperature range, the Zn sticking coefficient decreases with the increase in the growth temperature, while the Be sticking coefficient remains nearly constant.[12] Thus, we propose that the observed compositional variations may be due to small fluctuations of the substrate temperature during the growth.

The defect density of the epilayers was investigated by EPD measurements. A concentrated HCl solution (32%) was used. This solution has been previously reported to be a suitable defect revealing etchant for $Be_xZn_{1-x}Se$,

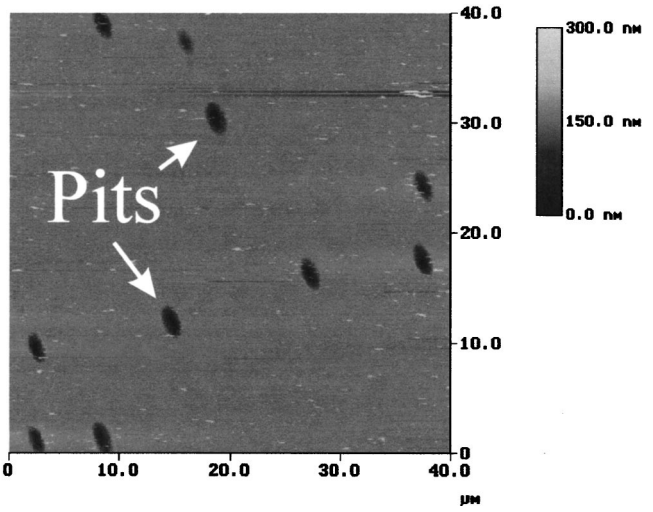

FIG. 3. Atomic force micrograph for a $Be_{0.51}Zn_{0.49}Te$ epilayer etched for 60 s in HCl (32%). Oval-shaped etch pits can be seen on the etched surface.

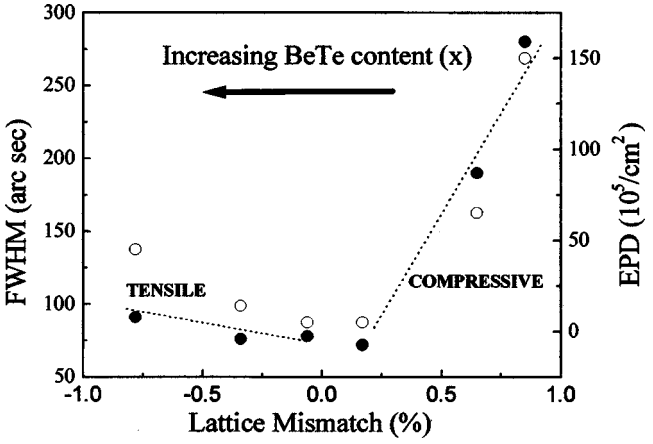

FIG. 4. FWHM of the x-ray rocking curves (solid circles) and etch pit density (open circles) for $Be_xZn_{1-x}Te$ epilayers as a function of lattice mismatch to InP. Dashed lines are drawn for ease of interpretation.

$Be_xMg_yZn_{1-x-y}Se$, and $Mg_xZn_{1-x}S_ySe_{1-y}$ alloys.[13–15] In our experiment, the etching behavior was examined by changing the etching time. The $Be_xZn_{1-x}Te$ layers were etched for 30, 60, 90, and 120 s and their surface was studied using Nomarski microscope and AFM. No defects are seen on the as-grown surface. When etched for 30 s, etch pits can be observed. With an increase in the etching time, the pits become bigger and deeper, but the density remains constant during the etching and does not depend on etch time. Figure 3 shows an AFM image ($40\times40\ \mu$m) of the $Be_{0.51}Zn_{0.49}Te$ epilayer after the etching for 60 s in HCl. The pits have an oval shape with a size of $3\times1\ \mu$m and are very deep, in excess of 150 nm. From studies of similar materials, these etch pits are expected to be related to defects in the II-VI layer, such as misfit dislocations and stacking faults.

The properties of the $Be_xZn_{1-x}Te$ epilayers grown in this study are summarized in Table I. In Fig. 4, the FWHM of the double-crystal x-ray rocking curves (solid circles) and the EPD values (open circles) for these epilayers are plotted as a function lattice mismatch ($\Delta a/a$) to the InP substrate. As the figure indicates, the epilayer quality decreases with the increase of the lattice mismatch, evidenced by the broadening of the x-ray rocking curves and the increase in the defect density. This is likely due to relaxation of the layer by the formation of misfit dislocations to accommodate strain. Furthermore, the FWHM of the x-ray rocking curves and the EPD values for the layers under tensile strain increase much more slowly with respect to lattice mismatch than for the epilayers under compressive strain. As shown in Table I, $Be_xZn_{1-x}Te$ layers under tensile strain have a higher Be content than those under compressive strain. An increase in the lattice hardness with increasing Be content has previously been reported for $Be_xZn_{1-x}Se$ and $Be_xZn_{1-x}Se_yTe_{1-y}$ alloys.[16,17] We interpret the different behavior for the layers under compressive and tensile stress by proposing that $Be_xZn_{1-x}Te$ layers with higher Be content can accommodate a larger misfit strain by elastic deformation without the formation of misfit dislocations, due to the expected increase in the lattice hardness.

TABLE I. Properties of $Be_xZn_{1-x}Te$ layers grown.

Composition	Mismatch (%)	FWHM (arcsec)	EPD (cm^{-2})	Thickness (nm)
$Be_{0.38}Zn_{0.62}Te$	0.85%	280	1.5×10^7	740
$Be_{0.4}Zn_{0.6}Te$	0.65%	190	6.5×10^6	690
$Be_{0.46}Zn_{0.54}Te$	0.17%	72	5×10^5	560
$Be_{0.51}Zn_{0.49}Te$	−0.06%	78	5×10^5	680
$Be_{0.53}Zn_{0.47}Te$	−0.34%	76	1.4×10^6	560
$Be_{0.58}Zn_{0.42}Te$	−0.78%	91	4.5×10^6	690

IV. CONCLUSION

We have investigated the MBE growth of $Be_xZn_{1-x}Te$ epilayers with different Be content on InP (100) substrates. A linear dependence of the Be content (in a log scale) on the Be (Zn) cell temperatures was observed indicating good control of the composition. Narrow x-ray rocking curves down to 72 arcsec with a low-etch pit density of mid-10^5 cm^{-2} were obtained for closely lattice-matched epilayers suggesting high-crystalline quality. Variations in $Be_xZn_{1-x}Te$ composition as a function of depth were observed in a few cases and attributed to small fluctuations of substrate temperature during the growth. $Be_xZn_{1-x}Te$ layers under tensile strain exhibited a slower rate of degradation as a function of the strain than layers under compressive strain. This was attributed to the enhanced lattice hardening in layers with higher Be content.

ACKNOWLEDGMENTS

The authors would like to acknowledge support from the National Science Foundation through Grant No. DMR 9805760. This work was done under the auspices of the Center for Advanced Technology on Ultrafast Photonics and the Center for Analysis of Structures and Interfaces.

[1]M. C. Tamargo, W. Lin, S. P. Guo, Y. Guo, Y. Luo, and Y. C. Chen, J. Cryst. Growth **214/215**, 1058 (2000).
[2]W. Faschinger and J. Nürnberger, Appl. Phys. Lett. **77**, 187 (2000).
[3]W. Shinozaki, I. Nomura, H. Shimbo, H. Hattori, T. Sano, S. B. Che, A. Kikuchi, K. Shimomura, and K. Kishino, Jpn. J. Appl. Phys., Part 1 **38**, 2598 (1999).
[4]W. Lin, B. X. Yang, S. P. Guo, A. Elmoumni, F. Fernandez, and M. C. Tamargo, Appl. Phys. Lett. **75**, 2608 (1999).
[5]S. B. Che, I. Nomura, W. Shinozaki, A. Kikuchi, K. Shimomura, and K. Kishino, J. Cryst. Growth **214/215**, 321 (2000).
[6]M. W. Cho, S. K. Hong, J. H. Chang, S. Saeki, M. Nakajima, and T. Yao, J. Cryst. Growth **214/215**, 487 (2000).
[7]O. Maksimov and M. C. Tamargo, Appl. Phys. Lett. **79**, 782 (2001).
[8]A. Cavus, L. Zeng, M. C. Tamargo, N. Bambha, F. Semendy, and A. Gray, Appl. Phys. Lett. **68**, 3446 (1996).
[9]M. W. Cho, J. H. Chang, S. Saeki, S. Q. Wang, and T. Yao, J. Vac. Sci. Technol. B **18**, 457 (2000).
[10]Landolt–Bornstein, *Numerical Data and Functional Relationships in Science and Technology*, edited by O. Madelung, H. Weiss, and M. Schulz (Springer, Berlin, 1982).
[11]T. Litz, H. J. Lugauer, F. Fischer, U. Zehnder, U. Lunz, T. Gerhard, H. Ress, and A. Waag, Mater. Sci. Eng., B **43**, 83 (1997).
[12]A. Waag, Th. Litz, F. Fischer, H. J. Lugauer, T. Baron, K. Schüll, U. Zehnder, T. Gerhard, U. Lunz, M. Keim, G. Reuscher, and G. Landwehr, J. Cryst. Growth **184/185**, 1 (1998).
[13]S. P. Guo, Y. Luo, W. Lin, O. Maksimov, M. C. Tamargo, I. Kuskovsky, C. Tian, and G. F. Neumark, J. Cryst. Growth **208**, 205 (2000).
[14]F. Fisher, M. Keller, T. Gerhard, T. Behr, T. Litz, H. J. Lugauer, M. Keim, G. Reuscher, T. Baron, A. Waag, and G. Landwehr, J. Appl. Phys. **84**, 1650 (1998).
[15]M. Shiraishi, S. Tomiya, S. Tanigachi, N. Nakano, A. Ishibashi, and M. Ikeda, Phys. Status Solidi A **152**, 377 (1995).
[16]F. C. Peiris, U. Bindley, J. K. Furdyna, H. Kim, A. K. Ramdas, and M. Grimsditch, Appl. Phys. Lett. **79**, 473 (2001).
[17]K. Mauyama, K. Suto, and J. Nishizawa, J. Cryst. Growth **214/215**, 104 (2000).